

Micro-resonance Raman study of optically trapped *Escherichia coli* cells overexpressing human neuroglobin

Kerstin Ramser

Göteborgs University
Department of Physics
SE-412 96 Göteborg, Sweden
and
Luleå University of Technology
Department of Computer Science and Electrical Engineering
SE-971 87 Luleå, Sweden
E-mail: kerstin.ramser@ltu.se

Wim Wenseleers

University of Antwerp
Department of Physics
Wilrijk-Antwerp, Belgium

Sylvia Dewilde

University of Antwerp
Department of Biomedical Sciences
Wilrijk-Antwerp, Belgium

Sabine Van Doorslaer

University of Antwerp
Department of Physics
Wilrijk-Antwerp, Belgium

Luc Moens

University of Antwerp
Department of Biomedical Sciences
Wilrijk-Antwerp, Belgium

Dag Hanstorp

Göteborgs University
Department of Physics
SE-412 96 Göteborg, Sweden

1 Introduction

Hemoglobins (Hb) can reversibly bind to dioxygen or other small ligands, and their main purpose is to transport oxygen to local tissues through the vascular system. The iron atom is the ligand binding site of the protein and is found in the heme prosthetic group. After binding of the iron atom to the proximal histidine residue, there is one remaining axial coordination site on the distal side available for ligand binding. The binding site is termed penta-coordinated if accessible for exogenous ligand binding, or hexa-coordinated if an amino acid side chain is connected to the site through an H-bridge. The main difference between the two forms is that biomolecular reactions are fast and straightforward in traditional penta-coordinate globins, whereas ligand binding to hexa-coordinated globins involves a competition between the exog-

Abstract. We describe the possibility of using a microresonance Raman spectrometer combined with a microfluidic system and optical tweezers to study *Escherichia coli* (*E. coli*) overexpressing wild type (wt) neuroglobin (NGB) and its E7Leu mutant, respectively. NGB is a recently discovered heme protein and its function still is a matter of debate. So far, the protein has been studied in its purified form, and *in vivo* measurements on the single cell level could give more information. To study the feasibility of the combined techniques, the possibilities of the setup are investigated by taking spectra from single cells and clusters of cells. We find that the microresonance Raman technique enables studies of the wt NGB protein in a living cell under fluctuating aerobic and anaerobic conditions. *E. coli* cells overexpressing wt NGB are stable, and the reversible oxygenation-deoxygenation can be studied over a long period of time. Further, the experiment indicates the presence of an enzymatic system in the bacteria reducing the ferric form NGB. The study of *E. coli* cells overexpressing E7Leu NGB, on the other hand, gives insight into limiting factors of the setup, such as cell lysis, photoinduced chemistry, and protein concentrations. © 2007 Society of Photo-Optical Instrumentation Engineers. [DOI: 10.1117/1.2753478]

Keywords: *E. coli* bacteria; neuroglobin; E7Leu neuroglobin; resonance Raman spectroscopy; optical tweezers; microfluidic systems.

Paper 06191RR received Jul. 24, 2006; revised manuscript received Apr. 18, 2007; accepted for publication Apr. 18, 2007; published online Jul. 24, 2007.

enous ligand and intramolecular coordination by the local amino acid (histidine) side chain. Thus, hexa-coordination is considered an alternative mechanism for regulating ligand binding to the heme, and new interest in the function structure relationship of heme proteins has begun.^{1,2}

A milestone within the heme-research was set in the year 2000 when Burmester et al. discovered a new mammalian globin predominantly expressed in the brain and therefore termed neuroglobin (NGB).³ Surprisingly, neuroglobin is the first mammal globin found to be in a hexa-coordinated low spin form both in the deoxy and oxy form, giving rise to many studies and suggestions on the still unknown function of the protein.⁴⁻²¹ The proposals are manifold: the globin might have a myoglobin-like function in the O₂ metabolism, and it may protect neuronal cells from hypoxic-ischemic insults.¹⁸ Also, it might function as an oxidative stress-responsive sensor protein, or participate in a signal transduction pathway that

Address all correspondence to: Kerstin Ramser, Tel: +46-920-491648; Fax: +46-920-493111, E-mail: kerstin.ramser@ltu.se, and Wim Wenseleers: Tel: +32-3-820.24.51, Fax: +32-3-820.24.70, E-mail: Wim.Wenseleers@ua.ac.be.

modulates activities of regulatory proteins in response to changes in O₂, CO, and NO concentrations. There is also the alternative of neuroglobin sustaining NO/O₂ scavenging and or reactive oxygen species (ROS) detoxification. It has also been found that oxygenation and carbonylation are linked to the redox state of the cell via intramolecular disulphide bridge formation/dissociation.¹⁰ However, the observations were made *in vitro* and no data are so far available about the physiological function of this disulfide bridge *in vivo*.²⁰

In the course of our previous studies on the NO-binding of neuroglobin proteins,^{5,22} we discovered that the oxidation of neuroglobin in cell lysates obtained from *E. coli* cells overexpressing neuroglobin is very slow in contrast to the fast autoxidation rate reported for these proteins.²³ Several *in vitro* experiments on the cell lysates strongly indicate the presence of an enzymatic system capable of reducing the ferric form of neuroglobin, and similar effects were observed in eukaryotic cells (data published elsewhere²⁴). For many of the biological relevant ligand-binding functions ascribed to globins, the reduction of the ferric globin is postulated to play an important role, although little or no information is available on the identity and *in vivo* working of the enzymatic systems that facilitate this reduction.²⁵ Our findings on the reduction of neuroglobin in *E. coli* as well as eukaryotic cells prompted us to investigate the possibility of observing the redox reaction in living cells, preferably on a single cell level, and thus probe directly the influence of changing external conditions, such as pH or oxygen levels, on the oxidation state of the globin. To enable *in vivo* measurements on the single cell level, we combined Raman spectroscopy with a microfluidic system and an optical trap.

Recently, we demonstrated how the combination of a micro-Raman spectrometer with a microfluidic system and optical tweezers can be used to study the oxygenation cycle of hemoglobin in optically trapped single red blood cells.²⁶ Resonance Raman spectroscopy is an excellent tool to investigate heme proteins. The resonance effect is strong enough to investigate the heme group without interference by surrounding media or other components of the sample, and therefore enabling whole cell studies.²⁷

Microfluidic systems are miniature structures of channels and reservoirs that give control over the diffusion of substances and chemical reactions in a confined space. They have become important tools in biomedicine and biochemistry, since they can mimic *in vivo* conditions in an *in vitro* environment.^{28–30} Such flow systems can easily be integrated into existing experimental setups due to their small sizes. Because of the flow, the cells under investigation need to be immobilized. Optical tweezers are ideal tools to avoid cell damage while guaranteeing stable immobilization of cells.³¹ The method is based on the fact that the photon momentum of light can be transferred onto small objects. A high gradient field close to a tightly focused Gaussian laser beam creates a force strong enough to trap micron-sized dielectric particles in three dimensions. Since the introduction of optical tweezers, they have become a significant tool in biochemistry.^{31–34}

Given the fact that the previously described approach of combining a microresonance Raman setup with optical tweezers and a microfluidic system holds promise for investigations on diverse heme-protein-containing cells,^{26,35} this method presents a possible strategy for tackling the earlier

mentioned observation of the redox processes in cells (over)expressing NGB. Ideally, the method should be used to observe NGB in eukaryotic cells. However, the protein is found in low concentrations in brain tissue³ and can therefore not be directly used for the experiment, since the blood hemoglobin corrupts the experimental results even for perfused brains. Furthermore, the culture of nerve cell lines is not straightforward and gives low yield. In this work, we therefore use *E. coli* bacteria overexpressing wild-type (wt) human NGB and its E7Leu mutant (His at position E7 substituted by Leu) to test the applicability and modifications of the microresonance Raman method. The choice of the system is also interesting in view of the earlier observation of the presence of an enzymatic system. The main adjustment to the technique is that the system now is equipped with a gas-tight flow cell coupled to a continuous pump. This gives the opportunity to vary the oxygen concentration in the buffer flushed through the gas-tight cell, which triggers oxygen release or binding of the heme.

As mentioned before, this method has previously proven to be feasible for studies of the oxygenation cycle of single red blood cells containing 33% of Hb and having a size of 100 μm^3 . The question we try to answer in this work is if it will hold to study single *E. coli* bacteria being about 100 times smaller with approximately 10 times less protein concentration. Therefore, part of the current study is dedicated to investigating the sensitivity of the setup, effects of laser power and optical trapping, and the possibility to visualize responses of the oxygenation state of the globin to environmental changes. The advantages and disadvantages of the technique are discussed. Finally, the current observations are linked to our earlier findings.

2 Materials and Methods

2.1 Setup

For this study, a home-built microscope equipped with a microfluidic system and optical tweezers were combined with a Raman spectrometer, as shown in Fig. 1. The flow cell used consisted of a flat Plexiglas ring ($\varnothing=5$ mm, $h=0.5$ mm) that was tightly sealed with vacuum grease between two cover glasses. The cell was flushed by a continuous pump connected to a switch leading to two buffer-containing vessels purged with air or N₂, respectively. This system enabled us to vary the aerobic conditions in the flow cell while simultaneously monitoring spectral changes. A Kr-ion laser tuned to 413.1 nm was used as an excitation source for the Raman measurements. The excitation and backscattering collection system consisted of an inverted microscope equipped with a 60 \times water-immersion objective (NA=1.2). The laser light was guided into the microscope by a dichroic mirror (DM1), reflecting 413.1 nm while transmitting the rest of the visible light. The Raman backscattered light was guided into a XY Dilor Raman spectrometer equipped (grating 1800 G/mm) by a second dichroic mirror (DM2), and thereafter passing a 10 \times objective to match the f ratio of the spectrometer entrance ($f/6$). The spectra were recorded by a liquid-nitrogen-cooled charge-coupled device (CCD) camera. Since the image of the laser focus in the sample is enlarged by the added optics, the variable slit in front of the resolving stage had to be open to pass the entire image, giving a calculated spectral resolution

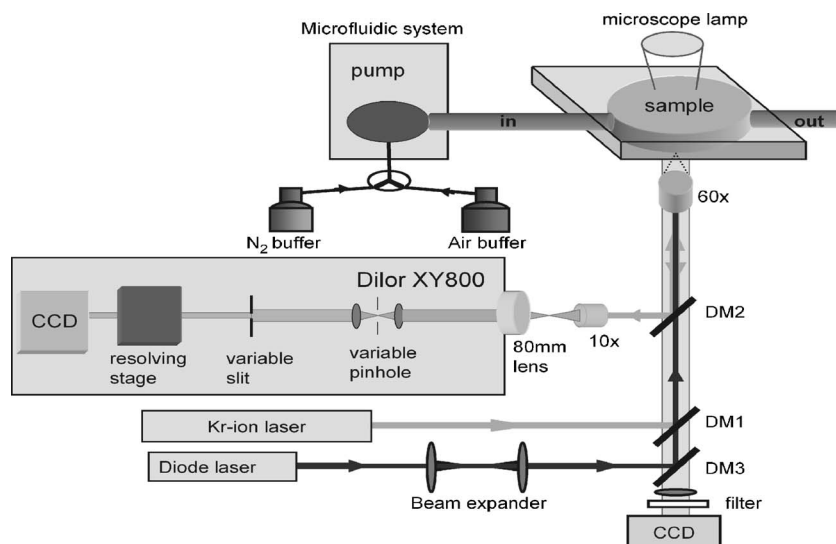


Fig. 1 Schematic of the setup. A Kr-ion laser tuned to 413.1 nm is used for Raman excitation. The excitation and backscattering collection system consists of an inverted microscope equipped with a 60× water-immersion objective (NA=1.2). DM1 leads the laser line into the microscope. The Raman backscattered light is guided into a Dilor XY800 Raman spectrometer by a second dichroic mirror (DM2), passing a 10× objective to match the f ratio of the spectrometer entrance. The trapping laser (830 nm) is guided by DM3 through the 60× microscope objective. A 1:5 beam expander is mounted in the trapping laser beam to assure stable trapping and to bring together the foci from the different lasers. The sample is monitored by a web camera. The microfluidic system, a Plexiglas ring ($\varnothing=5$ mm, $h=0.5$ mm) with an in- and outlet sealed between two cover glasses, is flushed with buffer by a continuous pump, equipped with a switch and connected to buffer containers (80 ml) purged with air or N_2 .

of 10 cm^{-1} . However, comparing spectra taken in the micro-configuration with the macroconfiguration (spectral resolution 3.5 cm^{-1}), no loss of spectral information could be observed. Hence, the calculated spectral resolution of 10 cm^{-1} might be overestimated.

The trapping laser (a diode laser emitting at 830 nm) was guided by a third dichroic mirror (DM3) through the 60× microscope objective used for the Raman setup and for the monitoring of the sample. Stable trapping was accomplished by overfilling the entrance aperture of the microscope objective. Therefore, a 1:5 beam expander was mounted in the light path of the trapping laser. The beam expander was also adjusted to get the focal point of the 413.1-nm beam and the 830-nm trapping laser to coincide. Safe visual observation/monitoring of the transmission microscopic image of the sample under white light illumination was accomplished using a CCD chip from a web camera coupled to a PC.

2.2 Sample

The growing of *E. coli* cells containing the expression plasmid encoding wt NGB or its E7Leu mutant has been described previously.⁷ Briefly, NGB cDNA cloned in pET3a were mutated using the QuickChange™ site-directed mutagenesis method (Stratagene), whereby the E7His was mutated to a Leucine (E7LeuNGB). The wt and mutant NGB expression plasmids (cDNA of NGB in pET3a) were transformed into *E. coli*, strain BL21(DE3)pLysS. The cells were grown at 298 K in TB medium (1.2% bactotryptone, 2.4 % yeast extract, 0.4 % glycerol, 72-mM potassium phosphate buffer pH 7.5) containing 200- $\mu\text{g}/\text{ml}$ ampicillin, 30- $\mu\text{g}/\text{ml}$ chloramphenicol, and 1-mM d-amino-levulinic acid. The culture was induced at $A_{550}=0.8$ by the addition of isopropyl-1thio-D-galactopyranoside of the final concentration of

0.4 mM, and expression was continued overnight.⁵ The fresh cells were washed and put in a suspension of the washing buffer (5-mM glucose, 25-mM Tris pH 8, and 10-mM EDTA). A drop of the cell suspension was put in the flow cell directly before the measurements started. The cell suspension was either taken directly from the batch (E7 LeuNGB) or diluted between 10^2 to 10^6 times (NGB), depending on the experiment.

3 Results

The first question addressed in this work was if it is possible to monitor single bacteria. In a previous study we showed that the microresonance Raman setup works very well to study the oxygenation cycle of hemoglobin in erythrocytes. However, red blood cells are large [typically 80 to $96\ \mu\text{m}^3$] and contain on average $300 \cdot 10^{-13}\text{ g}$ hemoglobin.³⁶ Considering that human hemoglobin contains four heme groups, the total heme concentration in erythrocytes is around 17 mM. *E. coli* cells are much smaller [typically $1\ \mu\text{m}^3$]³⁷ and the *E. coli* cells overexpressing NGB used in these experiments have, on average, globin (and hence heme) concentrations of around 2 to 4 mM. In a first step, we therefore compare the quality of resonance Raman spectra from different numbers of trapped *E. coli* cells overexpressing wt NGB. The concentration of cells was varied by altering the dilution from 10^2 and 10^3 to 10^6 . A drop of $100\ \mu\text{l}$ of the diluted bacteria suspension was put directly on a cover glass. The number of cells in the optical trap is determined from the optical microscopy image prior to switching to the Raman mode. Similarly, the cells were checked for lysis before and after illumination. Since the *E. coli* bacteria are known to lyse very fast after cell death, this can be used as a measure to determine whether the cells are still alive.

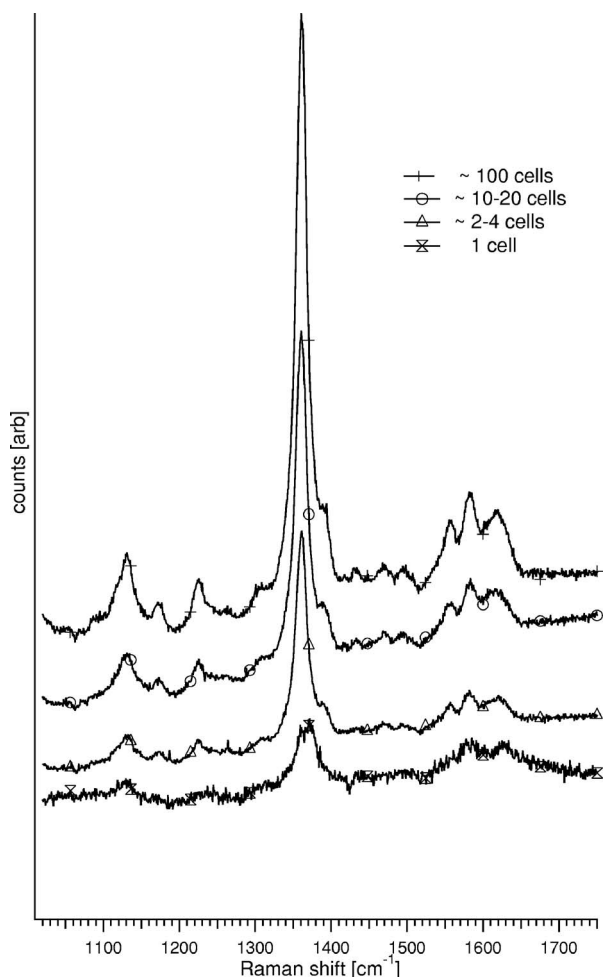


Fig. 2 Stacked spectra retrieved from different numbers of trapped *E. coli* bacteria overexpressing wt NGB. The setup can resolve spectra at the single cell level where the SNR increases with the number of cells trapped. The integration time was 120 s and the power, measured prior to the microscope objective, was 0.3 mW. The number of cells in the optical trap is determined from the optical microscopy image prior to switching to the Raman mode.

The results are depicted in Fig. 2, showing that the resolution of the setup is adequate to record resonance Raman spectra from a single, optically trapped bacterium. The signal increases with the number of trapped cells and is considerably lower when the optical trap is off. Remarkably, if only one cell is trapped, the signal decreases while the noise increases. This is due to the fact that the area of a single trapped bacterium ($\varnothing=1\ \mu\text{m}$) is smaller than the focused laser spot. Hence, also light reflected from the glass/water interface can be recollected. This is not the case when the whole measurement volume is filled with a dense population of cells. The ν_4 band at $1361\ \text{cm}^{-1}$, the iron oxidation state marker, is in all spectra the most dominant feature. When the optical trap and the flow are off, it is the only band detected, even with a high density of cells in the suspension (data not shown). The same is true if only a single or a few cells are trapped while a flow is applied through the flow cell. Using the optical trap to assemble a high density of cells within the Raman focus, the signal-to-noise ratio (SNR) of the spectra can be increased

substantially (Fig. 2). Even though ~ 10 to 20 cells should be sufficient to fill the laser spot in the focal xy plane, the signal continues to increase for a larger number of cells, mostly because of the contributions from other (out of focus) planes, as the focus of the laser beam is elongated along the z direction. During the initial test measurements, it was also found that only fresh cell suspensions gave a good SNR in the Raman spectra. This was clearly linked to the increasing cell lysis upon aging of the suspension. Furthermore, cell lysis is possibly enhanced under laser illumination and the level of cell disruption may in addition depend on the type of protein that is overexpressed in the cells, as is discussed later.

Secondly, we conducted an experiment where resonance Raman spectra of as-harvested *E. coli* cells were compared with spectroscopic data obtained earlier on the system and on the purified proteins. Previous studies, many of them involving some of the present coauthors, have led to a clear spectroscopic identification of neuroglobin and some of its mutants.^{4,5,7,16,20,22,38} Furthermore, both wt and E7Leu NGB are fully folded in the cytoplasm of the *E. coli* cells and are as such extracted from the cell lysate upon purification.⁷ We can therefore validate in detail the information obtained in our setup to probe possible corruption of the data by laser-induced processes.

Figure 3 (upper trace) shows the resonance Raman spectrum from *E. coli* cells overexpressing wt NGB. In this case, the washed cell suspension was diluted 50 times with buffer. In an earlier work, we showed that during protein expression in *E. coli*, the metabolism of the cells gradually shifts from aerobic to anaerobic respiration, since all available O_2 is consumed by the increasing population of cells.⁵ Nitrate reductase is then induced, causing nitrate to be reduced to nitrite and further to nitric oxide (NO). The *E. coli* cells under study are grown under these conditions. Using a combination of absorption spectroscopy and electron paramagnetic resonance (EPR), we proved earlier that wt NGB overexpressed in *E. coli* cell cultures favors the F8His- Fe^{2+} -E7His conformation, whereby only a small fraction of the protein binds NO.^{5,22} The present resonance Raman spectra taken from a group of optically trapped *E. coli* cells overexpressing wt NGB (upper trace, Fig. 3) confirm that the globin is in a reduced state, where no oxygen is bound to the heme, since the oxidation state marker ν_4 is found at $1361\ \text{cm}^{-1}$. The ν_3 band is found at $1493\ \text{cm}^{-1}$, confirming that the heme is in a hexacoordinated low spin form.^{4,38} Furthermore, the measured spectrum agrees well with earlier resonance Raman studies on the purified NGB, revealing that the globin is in its bis-histidine coordinated form in the deoxy ferrous state.⁴ The acquisition time in the experiment was set to 60 s per spectrum. In our previous absorption and EPR study, we showed that the nitrosyl ferrous form of E7Leu NGB is readily observed in *E. coli* cells overexpressing this mutant, since the competition with the distal histidine has now disappeared.^{5,22} Figure 3 (bottom trace) shows the resonance Raman spectrum of the trapped *E. coli* cells overexpressing E7Leu NGB. Fewer and broader bands are observed than in the previous case and a high fluorescence background is present. Also, the cell suspension is considerably less diluted ($4\times$) and more cells had to be trapped to get a sufficiently resolved Raman spectrum. This parallels the somewhat lower protein expres-

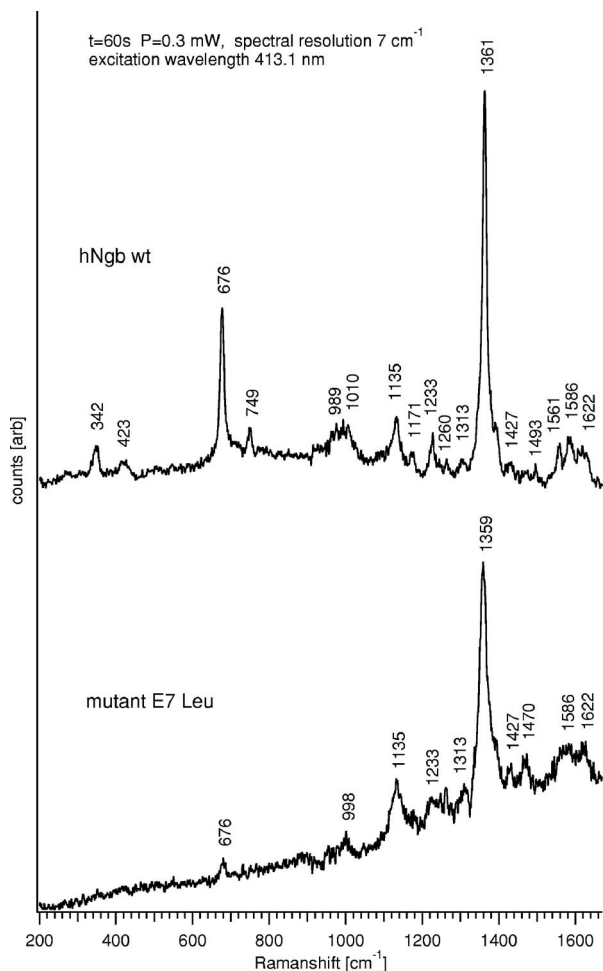


Fig. 3 Upper stacked spectrum shows typical ferrous Raman bands from 200 to 1660 cm^{-1} of wt NGB overexpressed in *E. coli* cells. The stacked spectrum below shows the same experiment for the E7Leu NGB. The integration time was set to 60 s at a power of 0.3 mW prior to the microscope objective.

sion in this case ($\sim 10\%$). Furthermore, the ν_4 band at 1359 cm^{-1} and the ν_3 band at 1470 cm^{-1} indicate that the heme is in the five-coordinated ferrous high-spin form as could be easily confirmed from a comparison with the resonance Raman spectrum of E7Leu NGB reduced with dithionite (not shown). This observation contrasts the EPR and absorption findings for these cell suspensions. This indicates that, besides the decreased stability of the *E. coli* cells against lysis (apparent from fluorescence background and visual cell lysis on microscope images), the local laser power is causing the Fe-NO bond to break (photochemistry). In contrast, the Fe-His bond is known to be far more stable against photodissociation. This experiment thus shows that photoinduced cell degradation and photodissociation can put a limit on the applicability of the technique and has to be monitored closely to avoid corruption in the interpretation of results.

In a third experiment, the influence of the cell environment on the globin was investigated. In our previous study, it was shown how the oxygenation process of a single erythrocyte under changing oxygen concentrations could be followed in time.²⁶ In the next step, we wanted to investigate if the envi-

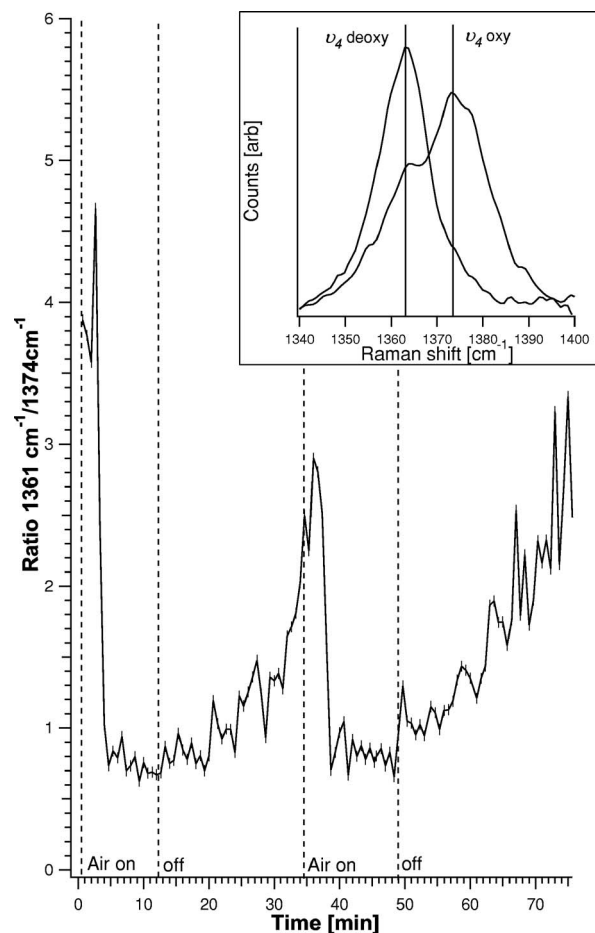


Fig. 4 Time series of the resonance Raman spectra of wt NGB overexpressed in *E. coli* cells. Raman laser power is 0.43 mW and the trapping laser power is 80 mW measured prior to the MO. Integration time is 40 s, and spectra are taken subsequently with no time delay. The graph shows the ratio between the ν_4 band at 1361 and 1374 cm^{-1} , respectively, giving a measure of the oxygen binding to the wt NGB. The inset shows the position of the ν_4 band for the oxy and the deoxy state from which the ratio was taken.

ronmentally induced changes of the oxidation/oxygenation state of the NGB variants could be monitored in *E. coli* cells. Therefore, the *E. coli* bacteria overexpressing wt NGB were exposed to a flow of air-purged buffer. Time series of spectra were taken to see how the bacteria react to environmental changes (Fig. 4). The power of the Raman excitation line at 413.1 nm into the microscope objective was measured to be 0.43 mW, whereas the power of the trapping laser (830 nm) was 40 mW. The optical trap assembled the cells at the focal point of the collection spot and kept the cells in place while the flow was applied. The integration time was set to 40 s, and the spectra were recorded subsequently with no time delay in between, to register spectral changes over time. It was possible to work with the same sample for 75 min without any photoinduced degradation of the sample or cell lysis. Approximately 20 cells were in the optical trap. The flow of the air-purged buffer (1 $\mu\text{l}/\text{min}$, flow-cell dimensions: $\varnothing = 5$ mm, $h = 0.5$ mm) was put on and off twice, while the subsequent shift of the ν_4 band in the resonance Raman spectra was recorded. When the cells are flushed with air-purged

buffer, the ν_4 band shifts from 1361 to 1374 cm^{-1} . $\nu_4 = 1361 \text{ cm}^{-1}$ identifies uniquely the reduced deoxy ferrous form of the globin, whereby $\nu_4 = 1374 \text{ cm}^{-1}$ agrees with both the oxy ($\text{His-Fe}^{2+}\text{-O}_2$) and the met (Fe^{3+}) form.⁴ The transfer between the forms is represented in Fig. 4 by the change in the ratio between the intensity values at 1361 and 1374 cm^{-1} .

The time span measured for the trapped cells to go from a clear deoxy state to a mixture between the deoxy and oxy form was around 2 min. When the flow was turned off, it took approximately 20 min for the cells to return to the reduced state again. From the graph, it can be seen that the cells are striving to be in the reduced state, and even when flushed with oxygen a pure oxy state is never observed in the spectra (data not shown). It is intriguing that wt NGB returns to a completely reduced state, although there should remain some oxygen in the flow cell, and the autoxidation rates are known to be very high from *in vitro* studies on purified NGB.⁷ Note that recorded time series of spectra of the *E. coli* did not reveal any photochemistry at the applied power.

The experiment was repeated for the *E. coli* cells overexpressing the E7Leu NGB mutant, giving a quite different result, as can be seen in Fig. 5. The results are worth presenting, since they show that great care has to be taken to avoid misinterpretation of the results retrieved with the applied technique.

The recorded spectra are taken from about 100 trapped *E. coli* cells in a very dense cell suspension, i.e., the cell suspension was not diluted from the beginning. The high density of cells in the trap was achieved by carefully collecting bacteria while scanning the sample. In this case, a flow of air-purged buffer was started after the recording of the second spectrum. The laser power was 0.3 mW. An immediate increase of the ν_4 band at 1374 cm^{-1} can be observed in Fig. 5. After three more spectra, this band disappears again for two spectra and then increases again. The disappearance of the 1374 cm^{-1} is accompanied by an increase in the signal-to-noise ratio. As mentioned before, the concentration of bacteria in the flow cell is very high to get a good signal; hence due to the flow, neighboring cells can be dragged into the focus of the trapping beam and give rise to the unexpected flipside shift of the ν_4 band. These fluctuations could also be observed on the microscope image. However, the decrease of the signal and the shift of the ν_4 peak to 1374 cm^{-1} imply that the sample is degrading quickly, despite of the access of fresh cells. This leads to the conclusion that when oxygen is abundant in the flow cell, the photoinduced degradation of the sample may even be accelerated. The observation that the Raman signal decreases significantly while the fluorescent background disappears over time is unexpected. As mentioned earlier, the *E. coli* bacteria overexpressing E7Leu NGB are extremely receptive to lysis, and only very fresh samples can be used in the experiments. Hence, the most likely explanation for the loss in signal, both Raman and the fluorescent background, is the ongoing lysis of the cells, which might be accelerated by the Raman-laser illumination, since the *E. coli* absorb significantly at 413.1 nm. Due to lysis, the content of the bacteria will diffuse into the flow cell instead of being assembled in the trapping focus. Further, it is obvious that the *E. coli* overexpressing the E7Leu NGB are more delicate and susceptible

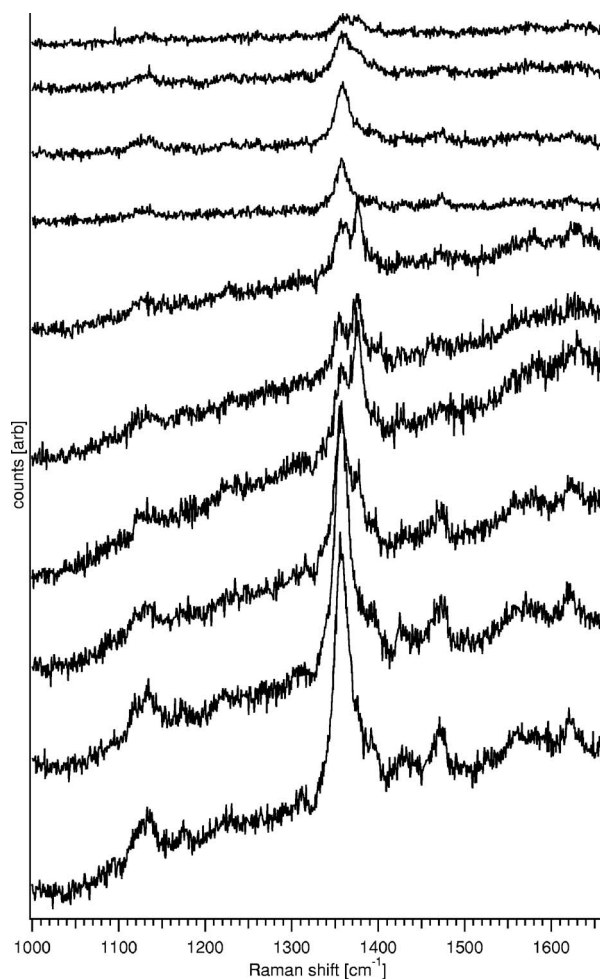


Fig. 5 Time series of stacked resonance Raman spectrum of NGBE7Leu overexpressed in *E. coli* cells. The first spectrum taken is shown at the bottom of the graph. Raman laser power is 0.3 mW and the trapping laser power is 40 mW measured prior to the microscope objective. The integration time is 40 s and spectra are taken in sequence with no time delay in-between. The flow starts after the second spectrum. An initial oxygenation is followed by a photoinduced degradation of the sample.

to photoinduced chemistry than *E. coli* overexpressing wt NGB.

4 Discussion

In a previous study, we presented the possibility of monitoring the oxygenation cycle of hemoglobin within single functional erythrocytes.²⁶ A double microscope configuration, equipped with two separate microscope objectives, was used to separate the optical trap from the Raman spectrometer. The reason for this was that the spectrometer was initially equipped with an upright microscope, and hence it was necessary to fine tune the optical conditions of each process individually to enable the integration of the microfluidic system. The method showed potential, but the oxygenation cycle was triggered by the addition of sodium dithionite, which resulted in a protein denaturation after one and a half cycles.^{26,27} In the present study, the spectrometer did not have a microscope integrated to start with, and hence an inverted microscope could be

added and the same objective could be used for optical trapping and the recording of Raman spectra. Furthermore, the flow through the gas-tight microfluidic system was generated by a continuous pump. This gives the possibility to switch between aerobic or anaerobic conditions, resembling physiological circumstances more than adding sodium dithionite into an open channel system. The time series presented in Fig. 4 shows that the state of the art equipment provides conditions that keep the cells functional over long periods of time, and hence it allows for the reversible monitoring of the oxygenation cycle of heme proteins.

The microfluidic system provides an ideal system to vary simultaneously or separately different aspects such as gas and salt concentrations and pH. In general, fluidic setups are required to be able to study continuously the influence of these varying circumstances, independently, whether one aims at a macroscopic or microscopic detection of the changes. Such a fluidic system implies fixation of the cells. The fixation of the cells using optical tweezers avoids cell damage that is known to occur when cells are immobilized to poly-lysine covered glass slides.²⁷ It allows, in combination with an optical microscope, for the selection and fixation of well-defined numbers of cells for the experiment, which is exactly the ultimate aim. The choice for a microscopic detection method is in this case evident. In comparison with absorption spectra, the resonance Raman spectra of globins are in principle richer in information. Moreover, the focusing of the laser light in resonance Raman is more optimal than the focusing obtained in a micro-absorption setup, where the large range of wavelengths needed for the experiment limits the focus characteristics. Therefore, the combined resonance Raman setup has in principle clear advantages over other techniques when observation of globin molecules in cells is targeted.

Here, it is demonstrated that the system is indeed suitable to study *E. coli* bacteria overexpressing NGB *in vivo* on the single-cell level, but the signal-to-noise ratio is low (Fig. 2). When the flow is started, the optical trap has to be applied not only to keep the cells in place but also to gather a high density of cells in the focus of the Raman beam to get good quality spectra. It has been demonstrated previously that optical trapping at 830 nm does not harm *E. coli* bacteria, and therefore it is an ideal immobilization tool, especially in combination with a microfluidic system.³³ The performance of the setup is limited by different factors. If the cell concentration in the suspension is too high, new cells can be dragged into the optical trap easily, corrupting the data in the time series (Fig. 5). Higher concentrations may, however, be necessary for cells with low protein expression needing a larger amount of cells in the trap to obtain a good quality spectrum. Furthermore, laser-induced cell lysis can put a limit to the applicability of the technique, and the trapped cells should be monitored by optical microscopy before and after the experiment. The approach can give insight on a cellular level, as is evident from the experiments on *E. coli* cells overexpressing wt NGB (Fig. 4).

As stated in the introduction, the current study was triggered by the discovery that an enzymatic system is present in *E. coli* and in eukaryotic cells that is capable of reducing NGB.²³ If we can develop a method that allows detection of the heme state of NGB in cells, we open the way of studying the behavior of the full NGB and enzyme system under vary-

ing conditions in a cell. To test the feasibility of using a micro-resonance Raman setup for these purposes, we focus in this study on the analysis of *E. coli* cells overexpressing wt NGB. In our *in vitro* studies, we found that the lysates of *E. coli* cells can reduce ferric wt NGB.²⁴ After the breaking of *E. coli* cells overexpressing wt NGB, an immediate formation of oxygenated wt NGB was observed due to the sudden presence of oxygen, but wt NGB was soon after found to return to the reduced state, despite the continuous exposure to air and despite the high autoxidation rate of NGB.⁷ Different experiments involving fractionation of the lysate, addition of trypsin or cofactors, showed unambiguously that the reducing agent is an enzyme.

The microresonance Raman experiments confirm that wt NGB is in a ferrous bis-histidine coordinated state in the *E. coli* cells grown under anaerobic circumstances, as was observed earlier^{5,22} (Fig. 3). Flushing with an oxygen-rich buffer induces the formation of oxygenated (or even oxidized) NGB, as could be determined from the shift of the ν_4 band (Fig. 4). However, based on the high autoxidation rate of NGB,⁷ one would expect at least partial oxidation of the NGB molecules in the cell. In contrast, when the oxygen flush is stopped, NGB is again reduced to the initial ferrous form. A full shift from the oxy form back to the deoxy form within 20 min after the stop of flow might be partially explained by the fact that the cells are consuming dioxygen at a high rate, but it cannot explain the lack of autoxidation of the protein under oxygen-rich conditions. The latter parallels the *in vitro* observations and shows that we have in principle a tool of measuring the coordination and oxidation state of globins.²⁴ However, to differentiate between the oxygenated and oxidized form of wt NGB, higher resolution resonance Raman spectra need to be taken, since the most prominent ν_4 and ν_3 bands do not allow for a differentiation between these forms. This implies an increase in measuring time and thus increases the time between spectra in a time series. Furthermore, the results can be corrupted by the technique itself, as became apparent from comparing the results on *E. coli* cells overexpressing wt NGB with those of the bacteria overexpressing E7 LeuNGB. Despite the fact that both proteins are not naturally abundant in the *E. coli* cell and may thus influence the host cell, and that in both cases the *E. coli* bacteria are found to be receptive to lysis, the lysis effect is considerably more pronounced for the *E. coli* cells overexpressing the E7Leu mutant than the wt globin. In the former case, even fresh samples show a high fluorescent background in the resonance Raman spectra, and many expected Raman bands cannot be resolved. The observation indicates that the cells are decomposing and the released DNA as well as the photodegradation of the heme give rise to the increased fluorescence. Furthermore, it is not possible to record spectral time series of these cells because of protein and cell degradation (Fig. 5). Our earlier absorption studies revealed that in *E. coli* cells overexpressing the NGB E7Leu mutant, the globin is found to be predominantly in a NO-ligated ferrous form.^{5,38} The local laser power needed for the present *in vivo* resonance Raman experiment is shown to dissociate the Fe-NO bond (Fig. 3). This will cause a sudden release of NO in the cell, which may well contribute to the higher receptivity to protein and cell degradation in compari-

son to the cells overexpressing the wt NGB, which is predominantly in the ferrous form. Furthermore, the NO-ligated ferrous forms of globins are known to absorb stronger at 413 nm than the bis-histidine coordinated ferrous form of heme proteins.²² This may induce a higher local heating of the cell, which again can contribute to the increased susceptibility to lysis of the cell. One should also note that the quantum efficiency for NO-ligated globins is in general lower than for O₂ or CO-ligated globins.³⁹ The current fast photodissociation is thus undoubtedly related to overall protein degradation due to lysis, and the formation of the ν_4 band at 1374 cm⁻¹ is thus most probably related to the formation of ferric heme. Apart from the susceptibility of the E7Leu mutant toward photoinduced chemistry, the high density of cells necessary for measurements causes problems. Fresh, close cells can be dragged into the optical trap, which can lead to a misinterpretation of the oxygenation state of the cells, especially when the flow is applied.

5 Conclusions

In conclusion, we show that a microresonance Raman spectrometer combined with optical tweezers and a microfluidic system allows for the reversible monitoring of oxygenation and redox cycles of heme proteins on a microscopic level in bacterial cells. This allows us to study not only the NGB system presented here under varying exposure of the *E. coli* cells to buffer purged with relevant ligands, but it also opens the way to study bacterial, *Archaea*, or eukaryotic globins in their native cells in the future. However, the present study also shows that photoinduced damage and low protein concentrations may put a serious limit to the method. These factors are system-bound and it is at all times necessary to monitor the validity of the data by checking the cells via optical microscopy and comparing the start and end point measurements with (macroscopic) absorption experiments.

Acknowledgments

This work was supported by the European Commission Sixth Framework Programme through the project ATOM-3D (contract number 508952), from the European Science Foundation EUROCORES Programme, SPANAS, through funds from the Swedish Research Council, and from the European Commission Sixth Framework Programme. Further acknowledgement goes to the Fund for Scientific Research-Flanders (FWO) for support through grant G.0468.03 and the postdoctoral fellowships granted to S.D. and W.W.. For technical assistance, we would like to thank Heinrich Riedl and Paul Casteels.

References

1. T. Egawa and S. R. Yeh, "Structural and functional properties of hemoglobins from unicellular organisms as revealed by resonance Raman spectroscopy," *J. Inorg. Biochem.* **99**, 72–96 (2005).
2. R. E. Weber and N. Vinogradov, "Nonvertebrate hemoglobins: functions and molecular adaptations," *Physiol. Rev.* **81**, 569–628 (2001).
3. T. Burmester, B. Welch, S. Reinhardt, and T. Hankeln, *Nature (London)* **407**, 520–523 (2000).
4. M. Couture, T. Burmester, T. Hankeln, and D. L. Rousseau, "The heme environment of mouse neuroglobin: evidence for the presence of two conformations of the heme pocket," *J. Biol. Chem.* **276**, 36377–36382 (2001).
5. S. Van Doorslaer, S. Dewilde, L. Kiger, S. V. Nistor, E. Goovaerts, M. C. Marden, and L. Moens, "Nitric oxide binding properties of

- neuroglobin," *J. Biol. Chem.* **278**, 4919–4925 (2003).
6. J. T. Trent, A. N. Hvitved, and M. S. Hargrove, "A model for ligand binding to hexacoordinate hemoglobins," *Biochemistry* **40**, 6155–6163 (2001).
7. S. Dewilde, L. Kiger, T. Burmester, T. Hankeln, V. Baudin-Creuz, T. Aerts, M. Marden, R. Caubergs, and L. Moens, "Biochemical characterization and ligand binding properties of neuroglobin, a novel member of the globin family," *J. Biol. Chem.* **276**, 38949–38955 (2001).
8. J. M. Kriegl, A. J. Bhattacharyya, K. Nienhaus, P. Deng, O. Minkow, and G. U. Nienhaus, "Ligand binding and protein dynamics in neuroglobin," *Proc. Natl. Acad. Sci. U.S.A.* **99**, 7992–7997 (2002).
9. D. Hamdane, L. Kiger, S. Dewilde, B. N. Green, A. Pesce, J. Uzan, T. Burmester, T. Hankeln, M. Bolognesi, L. Moens, and M. Marden, "The redox state of the cell regulates the ligand binding affinity of human neuroglobin and cytoglobin," *J. Biol. Chem.* **278**, 51713–51721 (2003).
10. E. Vinck, S. Van Doorslaer, S. Dewilde, and L. Moens, "Structural change of the heme pocket due to disulfide bridge formation is significantly larger for neuroglobin than for cytoglobin," *J. Am. Chem. Soc.* **126**, 4516–4517 (2004).
11. J. Uzan, S. Dewilde, T. Burmester, T. Hankeln, L. Moens, D. Hamdane, M. Marden, and L. Kiger, "Neuroglobin and other hexacoordinated hemoglobins show a weak temperature dependence of oxygen binding," *Biophys. J.* **87**, 1–7 (2004).
12. K. Nienhaus, J. M. Kriegl, and G. U. Nienhaus, "Structural dynamics in the active site of murine neuroglobin and its effects on ligand binding," *J. Biol. Chem.* **279**, 22944–22952 (2004).
13. S. V. Nistor, E. Goovaerts, S. Van Doorslaer, S. Dewilde, and L. Moens, "EPR-spectroscopic evidence for a dominant His-Fe^{III}-His coordination in ferric neuroglobin," *Chem. Phys. Lett.* **361**, 355–361 (2002).
14. A. Fago, C. Hundahl, S. Dewilde, K. Gilany, L. Moens, and R. E. Weber, "Allosteric regulation and temperature dependence of oxygen binding in human neuroglobin and cytoglobin," *J. Biol. Chem.* (2004).
15. J. T. Trent, R. A. Watts, and M. S. Hargrove, "Human neuroglobin, a hexacoordinate hemoglobin that reversibly binds oxygen," *J. Biol. Chem.* **276**, 30106–30110 (2001).
16. H. Sawai, M. Makino, Y. Mizutani, T. Ohta, H. Sugimoto, T. Uno, N. Kawada, N. Yoshizawa, T. Kitagawa, and Y. Shiro, "Structural characterization of the proximal and distal histidine environment of cytoglobin and neuroglobin," *Biochemistry* **44**, 13257–13265 (2005).
17. Y. Sun, K. Jin, X. O. Mao, Y. Zhu, and D. A. Greenberg, "Neuroglobin is up-regulated by and protects neurons from hypoxic-ischemic injury," *Proc. Natl. Acad. Sci. U.S.A.* **98**, 15306–15311 (2001).
18. S. Herold, A. Fago, R. E. Weber, S. Dewilde, and L. Moens, "Reactivity studies of the Fe(III) and Fe(II)NO forms of human neuroglobin reveal a potential role against oxidative stress," *J. Biol. Chem.* **279**, 22841–22847 (2004).
19. E. Geuens, S. Dewilde, D. Hoogewijs, A. Pesce, K. Nienhaus, G. U. Nienhaus, J. Olson, J. Vanfleteren, M. Bolognesi, and L. Moens, "Nerve globins in invertebrates," *IUBMB Life* **56**, 653–656 (2004).
20. S. Van Doorslaer, V. E. F. Trandafir, I. Ioanitescu, S. Dewilde, and L. Moens, "Tracing the structure-function relationship of neuroglobin and cytoglobin using resonance Raman and electron paramagnetic resonance spectroscopy," *IUBMB Life* **56**, 665–670 (2004).
21. A. Pesce, M. Bolognesi, A. Bocedi, P. Ascenzi, S. Dewilde, L. Moens, T. Hankeln, and T. Burmester, "Neuroglobin and cytoglobin: Fresh blood for the vertebrate globin family," *EMBO Rep.* **3**, 1146–1151 (2002).
22. F. Trandafir, S. Van Doorslaer, S. Dewilde, and L. Moens, "Temperature dependence of NO binding modes in human neuroglobin," *Biochim. Biophys. Acta* **1702**, 153–161 (2004).
23. F. Trandafir, S. Dewilde, L. Moens, and S. Van Doorslaer, "NO-binding properties and (non-)enzymatic reduction of human neuroglobin," *FEBS J.* **272**(Suppl. 1), (2005).
24. F. Trandafir, D. Hoogewijs, F. Altieri, P. Rivetti di Val Cervo, K. Ramser, W. Wenseelers, S. Dewilde, S. Van Doorslaer, J. Vanfleteren, and L. Moens, "Neuro- and cytoglobin as potential enzymes or substrates," *Gene* (in press).
25. M. Brunori, "Nitric oxide moves myoglobin centre stage," *Trends Biochem. Sci.* **26**, 209–210 (2001).
26. K. Ramser, J. Enger, M. Goksör, D. Hanstorp, K. Logg, and M. Käll, "A microfluidic system enabling Raman measurements of the oxy-

- generation cycle in single optically trapped red blood cells," *Lab Chip* **5**, 431–436 (2004).
27. K. Ramser, E. J. Bjerneld, C. Fant, and M. Käll, "Importance of substrate and photoinduced effects in Raman spectroscopy of single functional erythrocytes," *J. Biomed. Opt.* **8**, 173–178 (2003).
 28. G. M. Walker, H. C. Zeringue, and D. J. Beebe, "Microenvironment design considerations for cellular scale studies," *Lab Chip* **4**, 91–97 (2004).
 29. D. J. Beebe, G. A. Mensing, and G. M. Walker, "Physics and applications of microfluidics in biology," *Annu. Rev. Biomed. Eng.* **4**, 261–286 (2002).
 30. T. Fujii, "PDMS-based microfluidic devices for biomedical applications," *Microelectron. Eng.* **61-62**, 907–914 (2002).
 31. M. J. Lang and S. Block, "Resource Letter: LBOT-1: Laser-based optical tweezers," *Am. J. Phys.* **71**, 201–212 (2003).
 32. A. Ashkin, "History of optical trapping and manipulation of small-neutral particle, atoms, and molecules," *IEEE J. Sel. Top. Quantum Electron.* **6**, 841–856 (2000).
 33. K. C. Neuman, E. H. Chadd, G. F. Liou, K. Bergman, and S. Block, "Characterization of photodamage to *Escherichia coli* in optical traps," *Biophys. J.* **77**, 2856–2863 (1999).
 34. C. Kuyper and D. T. Chiu, "Optical trapping: a versatile technique for biomanipulation," *Appl. Spectrosc.* **56**, 300A–312A (2002).
 35. K. Ramser, K. Logg, M. Goksör, J. Enger, M. Käll, and D. Hanstorp, "Resonance Raman spectroscopy of optically trapped functional erythrocytes," *J. Biomed. Opt.* **9**(3), 593–600 (2004).
 36. G. B. Nash and H. J. Meiselman, "Red cell and ghost viscoelasticity. Effect of hemoglobin concentration and *in vivo* aging," *Biophys. J.* **43**, 63–73 (1983).
 37. T. E. Shehata and A. G. Marr, "Effect of temperature on the size of *Escherichia coli* cells," *J. Bacteriol.* **124**, 857–862 (1975).
 38. T. Uno, D. Ryu, H. Tsutsumi, Y. Tomisugi, Y. Ishikawa, A. J. Wilkinson, H. Sato, and T. Hayashi, "Residues in the distal heme pocket of neuroglobin: implications for the multiple binding steps," *J. Biol. Chem.* **279**, 5886–5893 (2004).
 39. W. A. Saffran and Q. H. Gibson, "Photodissociation of ligands from heme and heme proteins. Effect of temperature and organic phosphate," *J. Biol. Chem.* **252**, 7955–7958 (1977).